DEVELOPMENT OF ANALOG ELECTRONICS FOR THE BEAM LOSS MONITOR IN THE SUPERCONDUCTING SECTION OF THE CSNS II LINAC *

L. Zeng[1, 2], Z.J. Lu[1, 2], R.Y. Qiu[1, 2], F. Li[1, 2], Z. H. XU[1, 2], W.L. Huang[1, 2]
M.Y. Liu[1, 2], C.J. Xie[1, 2], R.J. Yang[†, 1, 2]
[1]Institute of High Energy Physics, Chinese Academy of Sciences (CAS), Beijing, China
[2]Spallation Neutron Source Science Center, Dongguan, China

Abstract

The China Spallation Neutron Source (CSNS) upgrade project has been launched on 2024, and aims to increase the beam power on the neutron target to 500 kW. A superconducting accelerating section will be constructed to boost the negative hydrogen beam energy from 80 MeV to 300 MeV. For the beam loss control and fast machine protection of the superconducting accelerator, the parallel-plate ionization chamber, which has been massively implemented to the Large Hadron Collider (LHC), will be employed. The beam loss monitor electronics is designed with an extremely wide measurement range (200 pA to 20uA) and requires a machine protection response time of less than 10 μs for major beam loss events. In this paper, two electronics schemes, current-to-voltage (IV) and current-to-frequency (IF) conversion analog circuits are designed and compared in detail. The beam test at the CSNS Linac is also reported.

INTRODUCTION

The power upgrade of the CSNS-II linear accelerator will adopt a superconducting acceleration structure, and the beam pipe will be located inside the cryogenic module, so the detection of beam loss can only be performed on the outer surface of the cryogenic module. The overall layout of the CSNS-II linac [1] is presented in Fig. 1. Due to the thick cavity, it has a significant shielding effect on the secondary radiation generated by beam loss. On the other hand, the need for superconducting quench protection requires a beam loss monitor (BLM) with faster response speed.

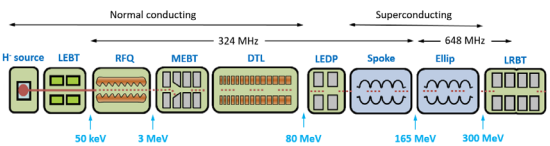

Figure 1: CSNS-II Linac layout.

CSNS-II accelerator plans to use parallel-plate multi-electrode ionization chambers as BLMs for its superconducting section, drawing on LHC BLM design in Fig. 2. This parallel-plate electrode BLM, critical for LHC [2], enhances sensitive volume and time response, and is widely used in ESS, GSI and other labs. A total of 45 such BLMs will be installed in the CSNS-II linac superconducting section.

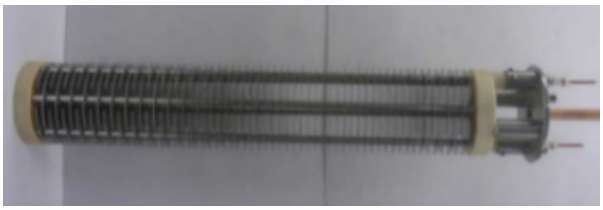

Figure 2: Parallel-plate ionization chamber.

The CSNS-II superconducting section BLM analog electronics conditions BLM detector output signals and provides interlock signals for machine protection, with detector, current range and electronics bandwidth similar to other mainstream international accelerators [3].

A comparison of BLM indicators of CSNS, ESS, SNS, LHC and FRIB shows none fully meet CSNS' needs: FRIB/LHC BLM beam abort response times are inadequate, other systems' hardware is incompatible with CSNS' planned platform, but their ionization chamber beam loss signal ranges are similar.

To measure such small pulse current signals, current amplification is needed to convert them into high-amplitude voltage/frequency signals. Mainstream international BLM front-end analog electronics fall into two types: ESS/SNS/FRIB's "current-to-voltage" (IV) conversion and LHC's "current-to-frequency" (IF) conversion.

IF CONVERSION

The IF conversion front-end analog circuit is designed with reference to LHC's beam loss electronics [4], consisting of an integrating amplifier, threshold comparison circuit, monostable circuit, and constant current discharge loop in Fig. 3. Its working principle: the detector's output current charges the integrating capacitor; during charging, the operational amplifier's output voltage decreases continuously. When it drops to the comparator's threshold voltage Vtr, the comparator triggers the monostable circuit, which outputs a fixed-width pulse to control the reference current source to discharge the capacitor. The total beam loss charge detected by the ionization chamber is accumulated as Qt at intervals T. The Machine Protection System (MPS) is generated by comparing the pulse counter's count with the calibrated unit-time count.

* Work Supported by National Natural Science Foundation of China (NO. 12305166) and the Natural Science Foundation of Guangdong Province, China, (NO. 2024A1515010016), Xie jialin's Grant (NO. E65461U2).
† yangrenjun@ihep.ac.cn

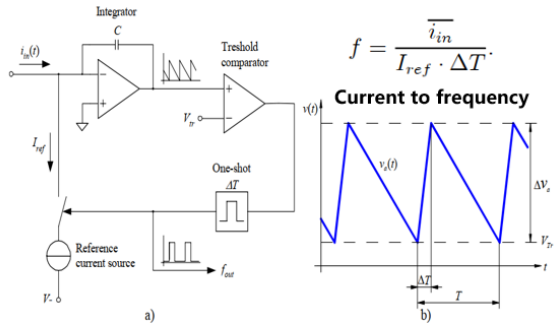

Figure 3: The block diagram of IF conversion.

The current-to-frequency conversion circuit has the advantages of ordinary integrating amplifier circuits. In addition, since its output signal is a pulse frequency signal, it has better anti-interference ability than voltage signals, which is conducive to long-distance transmission, and only an ordinary counter is needed to complete signal acquisition; the improvement of the charge-discharge circuit enables the I-F circuit to have no dead time limit, so it can accurately measure the cumulative output electric quantity of the detector. The schematic design of the IF signal conditioning circuit is shown in Fig. 4. The designed input signal range is 100 pA~300 μA, and the maximum output frequency is up to 5 MHz.

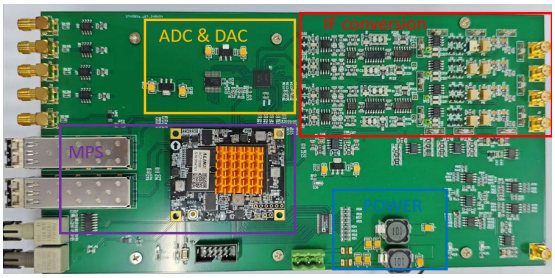

Figure 4: Photograph of the IF analog electronics.

IV CONVERSION

The IV conversion front-end analog circuit is designed with reference to the beam loss electronics of the Spallation Neutron Source (SNS) [5]. The circuit is composed of a first-stage variable gain amplifier circuit, a threshold comparison MPS circuit, a waveform display circuit, and a slow loss integration circuit, the block diagram of the principle is shown in Fig. 5. It linearly amplifies the current signal output by the ionization chamber into an output voltage signal. The electronic design has a current input range of 100 pA ~100 μA, and four gain levels are designed for the large dynamic range. The transimpedance of the 100 MΩ level is used to provide data for physicists under the requirements of small beam intensity and high beam loss resolution during beam tuning, while the 1 MΩ and other levels are used as a level for machine protection when the machine is in formal operation and large beam loss occurs, which fully meets the response time requirements during machine operation.

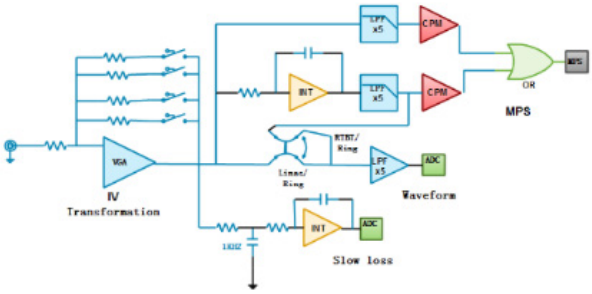

Figure 5: The block diagram of IV conversion.

Accelerator shutdown due to beam loss depends on macro-pulse dose accumulation or dose rate. For the former, an integration circuit integrates the first-stage IV conversion output, generates a comparison signal to compare with the set threshold for MPS signal; for the latter, the IV conversion output is directly compared with the threshold to generate MPS. Thus, the MPS circuit includes direct and integral comparison circuits: the integration circuit broadens ring and RTBT hundred-nanosecond waveforms to meet ADC acquisition requirements, with a lower MPS protection threshold for better machine protection. A waveform display circuit (5-fold gain, 100 kHz filtering) is designed for real-time beam loss display at each current position during tuning and operation. A slow loss circuit is added for beam loss that does not trigger immediate protection but causes equipment damage/activation over time: the signal passes through a 1 kHz low-pass filter and long-time integration, and the data acquisition system accumulates multi-cycle signals; software judges threshold excess, triggering beam shutdown and notifying physicists to optimize parameters. The IV conversion circuit schematic is shown in Fig. 6.

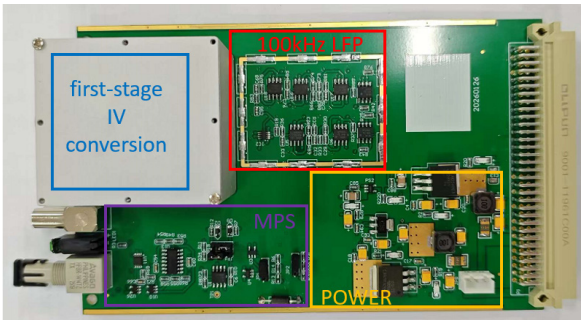

Figure 6: Photograph of the IV analog electronics.

BEAM-ON OPERATION TEST

To improve the sensitivity of the overall BLM system, the team is carrying out technological modification of the stacked ionization chamber and optimizing the selection of filling gas. In order to verify whether the performance of the BLM system can meet the engineering requirements for beam loss measurement and machine protection in the superconducting section, we adopted the wire of the LRWS in the CSNS I facility to block the beam at different positions [6]. When the wire is placed at the $\pm 3\sigma$ position , the intercepted beam current is approximately 100 nA, and the

beam loss signal can be clearly detected. The schematic diagram of beam blocking is shown in Fig. 7.

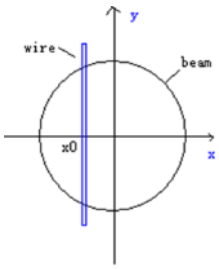

Figure 7: Schematic diagram of beam interception by a wire.

When the detection wire is placed at the beam center, the intercepted beam current is estimated to be approximately 0.1% of the total beam current.The parallel-plate ionization chamber is installed 1.8 meters behind the LRWS device, as shown in Fig. 8. The corresponding electronics are placed at the local beam measurement station, and the two are connected via a low-noise cable with a length of about 60 meters. Ionization chambers filled with nitrogen and xenon gases were tested in this work.

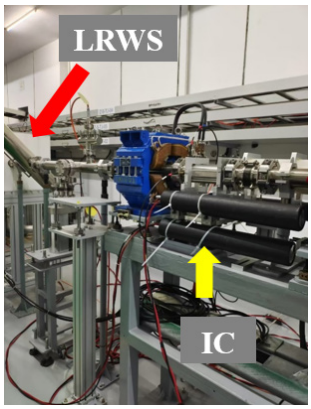

Figure 8: Layout of the ionization chamber and LRWS installation in the tunnel.

After testing, it is found that when the wire is located at the beam center, the IF conversion electronics can identify two consecutive pulses within 20 μs. The FPGA counts the number of pulses within the time window to determine and generate the MPS protection signal. The output waveform of the electronics is shown in Fig. 9.

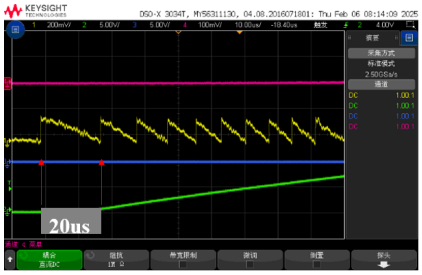

Figure 9: The output waveform of the IF electronics.

In the 1 M range of the IV conversion electronics, the signal amplitude of the xenon ionization chamber is significantly higher than that of the nitrogen ionization chamber. The measured rise time is 5.23 μs. By adopting an analog comparator circuit for threshold comparison, the MPS protection signal can be generated rapidly. Furthermore, the overall signal-to-noise ratio of the xenon ionization chamber is superior to that of the nitrogen ionization chamber. The output waveform of the electronics is shown in Fig. 10.

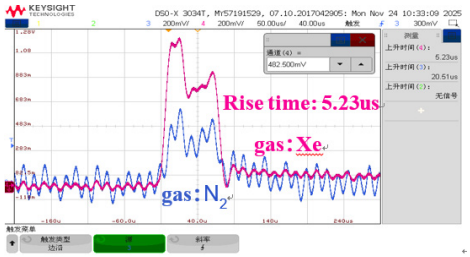

Figure 10: The output waveform of the IV electronics.

CONCLUSION

This paper has addressed the critical requirements for the CSNS-II superconducting section by investigating BLM analog electronics for hadron accelerators. Through comparative beam loss experiments conducted on the CSNS LRWS, the IV conversion electronics were selected as the baseline over the IF scheme. Although the IF design offers superior noise immunity, the IV scheme demonstrates a significantly faster rise time, which not only confirms its higher sensitivity but also ensures compliance with the stringent <10 μs MPS response requirement. Furthermore, detector optimization has been finalized with xenon selected as the fill gas for the ionization chambers, owing to its excellent signal-to-noise ratio.

REFERENCES

[1] R. J. Yang *et al.*, “Progress of the beam instrumentation development for the CSNS upgrade,” presented at ICFA Beam Dynamics Workshop (HB2025), Huizhou, China, Oct19, 2025.

[2] M. Stockner, B. Dehning, C. Fabjan, E. B. Holzer, and D. K. Kramer, “Classification of the LHC BLM Ionization Chamber”, in *Proc. DIPAC'07*, Venice, Italy, May 2007, paper WEPC09, pp. 328-330. doi:10.18429/JACoW-IPAC2023-PAPERID

[3] L. Tchelidze, H. Hassanzadegan, A. Jansson, and M. Jarosz, “Beam Loss Monitoring at the European Spallation Source”, in *Proc. IBIC'13*, Oxford, UK, Sep. 2013, paper WEPC45, pp. 795-798. doi:10.18429/JACoW-IBIC2013-WEPC45

[4] E. Effinger *et al.*, “The LHC beam loss monitoring system’s data acquisition card,” in *Proc. 12th Workshop on Electronics for LHC and Future Experiments*, Valencia, Spain, Sep. 2006.

[5] R. Witkover *et al.*, “Preliminary Design of the Beam Loss Monitoring System for the SNS”, in *10th Beam Instruction Workshop*, pp. 392-395, 2002. doi:10.1063/1./342610

[6] J. L. Sun *et al.*, “Study with Wire Scanner and Beam Loss Monitor at CSNS-LINAC”, in *Proc. IPAC'19*, Melbourne, Australia, May 2019, pp. 2598-2601. doi:10.18429/JACoW-IPAC2019-WEPGW053